Pergamon

Int. J. Solids Structures Vol. 32, No. 19, pp. 2853–2871, 1995

0020-7683/95 $9.50 + .00

0020-7683(94)00267-3

# MULTIPLE CRACKING IN FUNCTIONALLY GRADED CERAMIC/METAL COATINGS

G. BAO and L. WANG
Department of Mechanical Engineering, The Johns Hopkins University, Baltimore, MD 21218, U.S.A.

(*Received* 8 *August* 1994; *in revised form* 26 *October* 1994)

**Abstract**—Functionally graded coatings such as thermal barrier coatings on advanced metals and alloys can sustain multiple cracking upon thermal and mechanical loading. A special feature pertaining to the fracture behavior of coating is the coating gradation which can be characterized by the local volume fraction of metal. To guide the design of coating gradation so that cracking damage can be minimized, a fracture mechanics study is made of the crack driving force for multiple cracks in functionally graded ceramic/metal coatings. The metal substrate and the ceramic/metal coating are taken as linear elastic, with the elastic properties of the coating varying through the film thickness. Systematic finite element calculations are made for the energy release rate of the cracks in the coating as determined by the coating gradation, crack length, and the crack density; both mechanical and thermal loads are considered. It is found that compared with the pure ceramic coating, gradation of the coating can significantly reduce the crack driving force. It is also found that under mechanical loading the effect of different gradations on the crack driving force is relatively small. However, under thermal loading the influence of coating gradation can be significant. The implications of the results for the material design of functionally graded coatings are discussed.

## 1. INTRODUCTION

A functionally graded material (FGM) is a composite whose composition varies from place to place according to performance requirements. Recent development of FGM has demonstrated that such materials have the potential to enjoy a wide range of thermal and structural applications including thermal gradient structures, wear and corrosion resistant coatings and metal/ceramic joining (Takahashi and Hashida, 1990). For example, the use of functionally graded thermal barrier coatings can significantly reduce thermal residual stresses responsible for interface delamination and film spalling damage (Niini *et al.*, 1987). Functional gradation opens a new avenue for optimizing both material and component structures to achieve high performance and material efficiency. At the same time, it posts many challenging mechanics problems, including the prediction and measurement of the effective properties, thermal stress distributions and fracture of FGMs.

In the quest for the solution of these problems and for establishing the fundamental relationship between material gradation and thermomechanical properties of FGMs, extensive studies have been carried out, both theoretically and experimentally, on thermal stress distribution (Drake *et al.*, 1993; Williamson *et al.*, 1993; Giannakopoulos *et al.*, 1994) and fracture (Delale and Erdogan, 1983, 1988; Erdogan, 1985; Erdogan and Wu, 1993) in functionally graded materials. Micromechanics models for the effective properties of certain types of FGMs have also been developed (Aboudi *et al.* 1994; Zuiker and Dvorak, 1994). Pioneered in mechanics analysis of FGMs, Erdogan and coworkers have solved some basic fracture mechanics problems for a single crack in nonhomogeneous elastic materials under mechanical loads. Their work has been extended by Noda and Jin to include thermal load (Noda and Jin, 1993; Jin and Noda, 1993a,b; 1994a,b). Experimental observations of cracking in FGMs have been made by several investigators, including multiple cracking in a NiAl–$Al_2O_3$ FGM layer under bending (Lannutti, 1994). The present study focuses on multiple cracking in coating/substrate systems under thermal and mechanical loads.

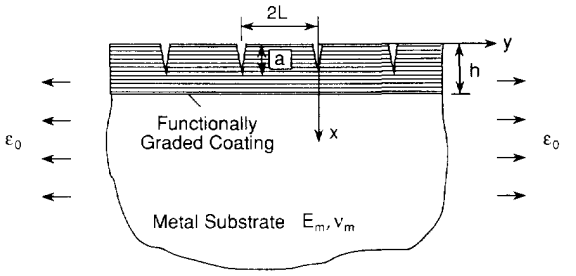


Fig. 1. A schematic of multiple cracking in a functionally graded coating/metal-substrate system.

Ceramic, metal and polymer coatings have been widely used in various industries, from aerospace to automobile to microelectronics, to enhance performance. In particular, ceramic coatings have been developed for use in thermal gradient structures, automotive engines and cutting and grinding tools to protect the surfaces from melting, wear, corrosion and oxidation. However, owing to thermal expansion mismatch between the coating and substrate, multiple cracking and coating spalling can occur upon experiencing thermal cycling and mechanical loading, causing premature failure of the component. The use of functionally graded coatings has the potential to simultaneously reduce thermal expansion mismatch, increase interface bonding strength, and enhance coating toughness. To realize this potential, a systematic micromechanics study is carried out in this paper on multiple cracking in a functionally graded ceramic/metal coating deposited on a metal substrate, as shown schematically in Fig. 1. Emphasis in this study is placed on establishing the link between the fracture behavior of the coating material and its gradation, aiming to providing guidance to both the coating design and the life prediction of the FGM coating/substrate systems.

Multiple cracking in the coating is a common damage mechanism in many coating/substrate systems (Gecit, 1979; Hu and Evans, 1988). Under inplane tensile stressing, the first set of cracks form from initial flaws and grow in a channeling fashion (Hutchinson and Suo, 1992). With further increase of the loading, more cracks are nucleated and propagate in between the existing channels. The crack spacing, however, usually attains a saturation value due to interactions of neighboring cracks and the relief of the tensile stress in the coating. Similar cracking scenario can be found in the growth of transverse cracks in brittle matrix composites (Varna and Berglund, 1994; Wang, 1984; Wang *et al.*, 1984). Although the coating material in the above-mentioned studies is homogeneous, it is expected that similar features remain true in the fracture of FGM coatings.

In this paper, the functionally graded ceramic/metal coating is assumed to be perfectly bonded to the homogeneous, isotropic metal substrate. The coating is taken to be a composite with the local volume fraction of metal varying through the coating thickness, mimicking an inclusion/matrix type FGM shown in Fig. 2a, or a FGM multilayer depicted in Fig. 2b. Both the FGM coating and the substrate are taken as linear elastic; plasticity of the metal phase as well as possible crack bridging mechanisms are neglected in the

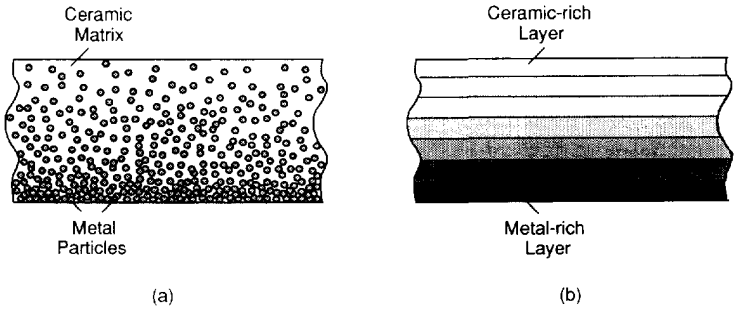


Fig. 2. Typical microstructures of functionally graded coatings. (a) An inclusion/matrix structure and (b) a multilayered structure.

present study. The metal/ceramic gradation in the FGM coating is taken to be of a power-law type; linear and nonlinear distributions of the metal phase in the coating are considered. The coating/substrate system is subjected to mechanical loading, or thermal loading, or a combination of the two. Systematic predictions for the crack driving force of multiple cracks in the coating are made using finite element analysis. These predictions can provide guidance to the gradation design of functionally graded materials.

## 2. COATING GRADATION

Based on the performance requirements for thermal barrier coatings and coatings in wear-related applications, in this study, only coatings that are ceramic-rich near the surface and metal-rich near the interface are considered. For convenience, the $x$-axis is set along the coating thickness direction, the $y$-axis lies within the coating surface, as illustrated in Fig. 1. At any position $x$ in the ceramic/metal coating, the local volume fraction of metal is assumed to be $g(x)$ which can be used to characterize the coating gradation. Generally speaking, $g(x)$ can be any non-singular, non-negative function of $x$. To gain insight into the effect of material gradation on the fracture behavior of a FGM coating, it is assumed that the local volume fraction of metal $g(x)$ obeys a power-law type relation

$$g(x) = g_0 + (1 - g_0)(x/h)^n, \tag{1}$$

where $g_0$ and $n$ are material parameters. The gradation given in eqn (1) implies that the coating always has 100% metal at the interface (i.e. $g(h) = 1$) which is, of course, desirable. Though idealized, the coating gradation defined in (1) can be used to model FGM coatings of both the inclusion/matrix type shown in Fig. 2a, and the multilayered type shown in Fig. 2b.

The total volume fraction $f$ of metal in the coating is given by

$$f = \frac{1}{h}\int_0^h g(x)\,\mathrm{d}x. \tag{2}$$

The parameter $g_0$ is thus related to $f$ and $n$ by

$$g_0 = [(n+1)f - 1]/n. \tag{3}$$

Obviously, $g_0$ cannot be negative for it is the metal volume fraction at the coating surface ($x = 0$). This sets a restriction on the values that $n$ could take for any given $f$. For example, if $f = 0.5$, we must have $n \geqslant 1$. If, in addition to $g(h) = 1$, we require that $g(0) = 0$, i.e. the material at coating surface is pure ceramic, then

$$g_0 = 0. \tag{4a}$$

In this case, $g(x)$ is a pure power-law function of $x$

$$g(x) = (x/h)^n \tag{4b}$$

and the total volume fraction $f$ of metal in the coating and the exponent $n$ in eqn (4b) are related by

$$f = 1/(n+1). \tag{5}$$

The coating gradation given in eqn (4b) is similar to that used by Drake *et al.* (1993) in their study of thermal residual stresses in FGM systems.

In what follows, two systems of coating gradation will be considered. In the first system, the total volume fractions of metal and ceramic in the coating are taken to be equal,

i.e. $f = 0.5$, and the exponent $n$ is assumed to be 1, 2, 3, 4 and 5, as illustrated in Fig. 3a. The corresponding values of $g_0$ are given by eqn (3). In the second system, the coating is assumed to have 100% ceramic at the surface ($x = 0$). The exponent $n$ is taken to be 0.5, 1 and 2 as shown in Fig. 3b, with the total volume fraction of metal $f$ given by eqn (5).

Owing to the heterogeneous nature of functional gradation, it is quite difficult to obtain the effective elastic moduli and thermal expansion coefficient of a FGM coating from the relative volume fractions and thermomechanical properties of the metal and ceramic phases. For a FGM coating of the inclusion/matrix type (Fig. 2a), the microgeometry of each phase is usually irregular, the spatial distribution of the phases is not uniform along the $x$-direction, and the homogenization can only be made within a plane perpendicular to the $x$-axis. Consequently, the existing micromechanical cell models are no longer valid in this case since no unit cell containing a single particle can be used to represent the whole composite body. Even if one chooses a unit cell containing many particles aligned along the coating thickness, due to the finite thickness of the coating, there is a particle-size dependence of the unit cell. For a FGM with a layered structure as that depicted in Fig. 2b, the existing micromechanical cell models are valid only if the thickness of each individual layer is much larger than the average particle size. A robust micromechanical model for the thermomechanical properties of a functionally graded composite has yet to emerge.

As a first order approximation, the effective properties of a functionally graded material can be obtained using the rule of mixtures. Specifically, the effective Young's modulus $E(x)$ for an inclusion/matrix type FGM coating can be given by

$$E(x) = g(x)E_m + \{1 - g(x)\}E_c \tag{6a}$$

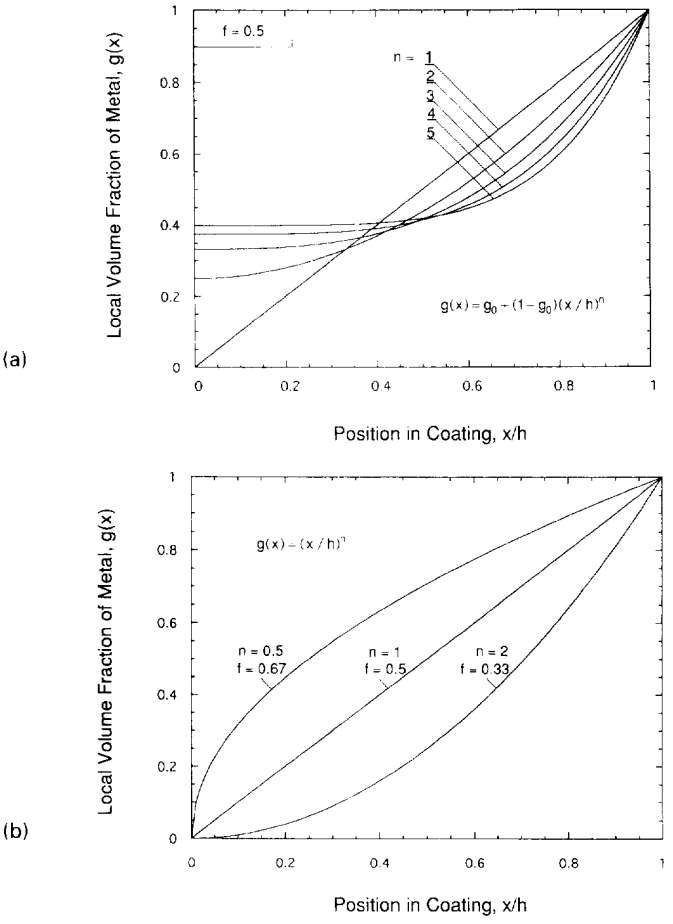


Fig. 3. Systems of coating gradation considered in the study. (a) The local volume fraction of metal $g(x)$ obeys eqn (1) with $f = 0.5$, $n = 1$, 2, 3, 4 and 5; (b) $g(x)$ is defined by eqn (4b) with $n = 0.5$, 1, and 2.

as the upper bound or

$$1/E(x) = g(x)/E_m + \{1-g(x)\}/E_c \tag{6b}$$

as the lower bound where $g(x)$ is the local volume fraction of metal defined in eqn (1), and $E_m$ and $E_c$ are Young's moduli for the metal and ceramic phase, respectively. Similarly, the effective Poission's ratio $v(x)$ and thermal expansion coefficient $\alpha(x)$ for the coating can be given respectively by

$$v(x) = g(x)v_m + \{1-g(x)\}v_c \tag{7}$$

and

$$\alpha(x) = g(x)\alpha_m + \{1-g(x)\}\alpha_c, \tag{8}$$

where $v_m$ and $v_c$ are Poission's ratios and $\alpha_m$ and $\alpha_c$ are thermal expansion coefficients for the metal and ceramic phase, respectively. Though very simple to use, the accuracy of the rule-of-mixtures solutions cannot be established.

An alternative approach is to obtain thermomechanical properties of a FGM coating using micromechanics models developed for composites with homogeneously distributed reinforcements. For example, taking the FGM coating shown in Fig. 2a as a spherical particle reinforced metal/ceramic composite, the effective bulk modulus of the coating can be expressed as (Hashin, 1962)

$$k(x) = k_m + \frac{[1-g(x)](k_c-k_m)}{1+g(x)[(k_c-k_m)/(k_m+\frac{4}{3}\mu_m)]}, \tag{9}$$

where $k_m$ and $k_c$ are bulk modulus for metal and ceramic, respectively, and $\mu_m$ is the shear modulus for the metal phase. The effective shear modulus of the coating can be solved from (Christensen and Lo, 1979)

$$A\left[\frac{\mu(x)}{\mu_m}\right]^2 + B\left[\frac{\mu(x)}{\mu_m}\right] + C = 0, \tag{10}$$

where $A$, $B$ and $C$ are functions of $g(x)$, $\mu_c/\mu_m$, $v_c$ and $v_m$ given in Christensen and Lo (1979), and $\mu_c$ is the shear modulus for the ceramic phase. The effective Young's modulus $E(x)$ and Poission's ratio $v(x)$ are given in terms of $k(x)$ and $\mu(x)$ by

$$E(x) = \frac{9k(x)\mu(x)}{3k(x)+\mu(x)}, \quad v(x) = \frac{E(x)}{2\mu(x)} - 1. \tag{11}$$

Finally, the effective thermal expansion coefficient $\alpha(x)$ for the coating is given by (Christensen, 1991)

$$\alpha(x) = \alpha_m + \frac{(\alpha_c-\alpha_m)}{(1/k_c-1/k_m)}\left[\frac{1}{k(x)} - \frac{1}{k_m}\right]. \tag{12}$$

Clearly, owing to material gradation, the effective elastic moduli and thermal expansion coefficient for the coating obtained above are only approximations even if the particles can

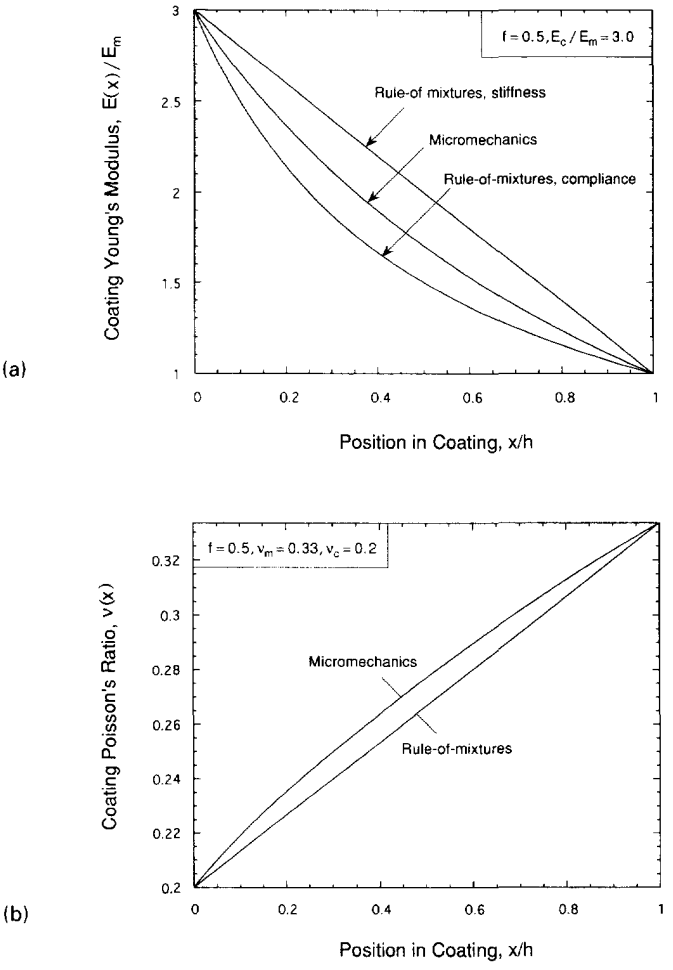


Fig. 4. Comparison of the effective elastic moduli of the coating given by the rule-of-mixtures solution and by the micromechanics solution. (a) Young's modulus $E(x)/E_m$ and (b) Poission's ratio $v(x)$.

be taken as spherical. However, it is believed that these solutions are better than the rule-of-mixtures solutions given in eqns (6)–(8). To drive this point home, in Fig. 4a, the effective Young's modulus $E(x)$ is normalized by $E_m$ and plotted as a function of the position in the coating $x/h$ for $f = 0.5$, $n = 1$, $E_c/E_m = 3$ using eqns (6a), (6b) and (9)–(11). It is seen that the micromechanics solution given by eqns (9)–(11) falls inbetween the rule-of-mixtures solutions (6a) and (6b) which are upper and lower bounds; the true solution, whatever it is, should also fall inbetween solutions (6a) and (6b). It can, therefore, be expected that the micromechanics solution for $E(x)$ is closer to the true solution compared with those given by eqns (6a) and (6b). Shown in Fig. 4b is a comparison of the effective Poission's ratio for the coating $v(x)$ given by the micromechanics solution (9)–(11) and the rule-of-mixtures solution (7). Here again, it is believed that the micromechanics solution for $v(x)$ is more accurate, although no rigorous proof can be given.

To illustrate the dependence of the effective elastic moduli and thermal expansion coefficient given by eqns (9)–(11) on the coating gradation $g(x)$, in Fig. 5a, $E(x)$ is normalized by $E_m$ and plotted against the position in the coating $x/h$ for $f = 0.5$, $E_c/E_m = 3$, $v_m = 1/3$, $v_c = 0.2$ for $n = 1$, 2, 3, 4 and 5. Similar plots are displayed in Fig. 5b for the effective Poission's ratio $v(x)$ and in Fig. 5c for thermal expansion coefficient $\alpha(x)$ of the FGM coating for $\alpha_m = 1.3 \times 10^{-5}/^{\circ}C$, $\alpha_c = 0.8 \times 10^{-5}/^{\circ}C$. The elastic moduli and thermal expansion coefficients are chosen from a $TiAl/Al_2O_3$ metal/ceramic composite but the results can be applied to other composite systems with similar material property combinations. Clearly, the nonlinearity of the functions $E(x)$, $v(x)$ and $\alpha(x)$ is similar to that of $g(x)$, but

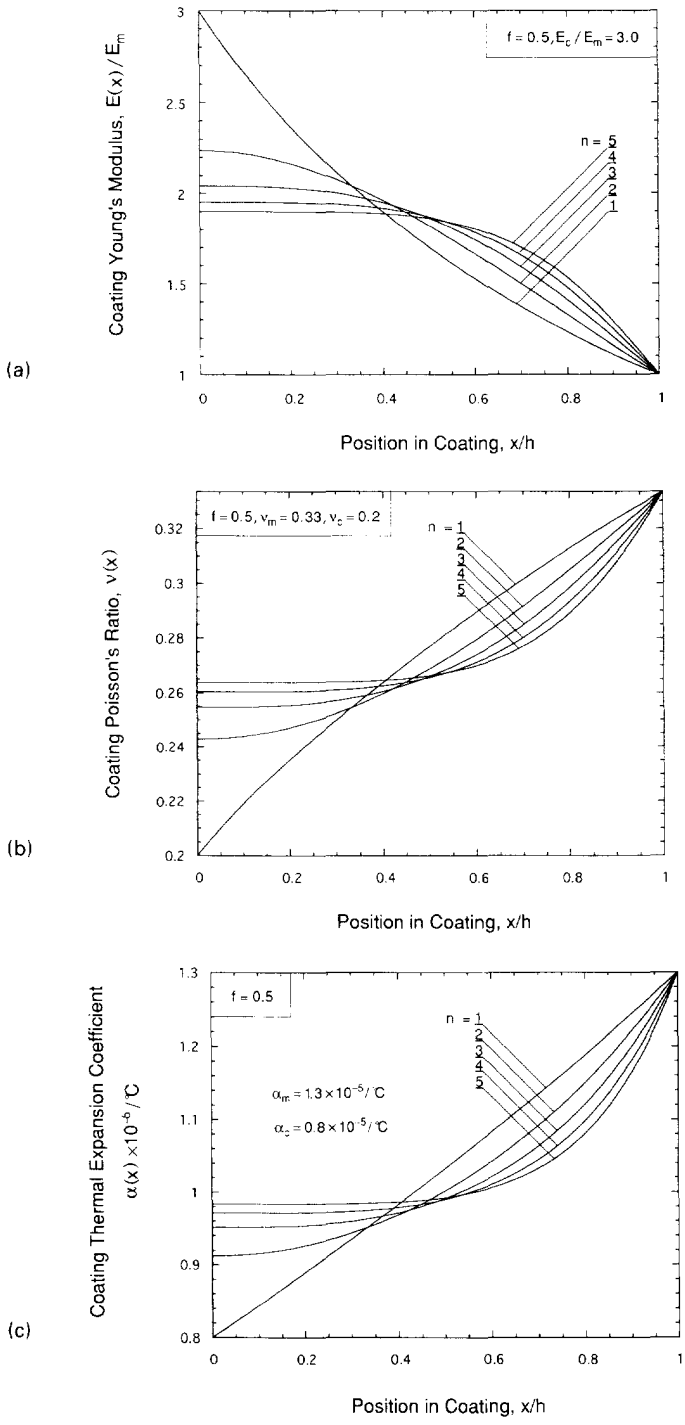


Fig. 5. Dependence of the effective elastic moduli and thermal expansion coefficient of the coating on the coating gradation $g(x)$ given in eqn (1). (a) Young's modulus $E(x)/E_m$; (b) Poission's ratio $\nu(x)$ and (c) thermal expansion coefficient $\alpha(x)$.

even if $g(x)$ is a linear function of $x$ as in the case of $n = 1$, $E(x)$, $\nu(x)$ and $\alpha(x)$ are nonlinear which is in contrast with the rule-of-mixtures solutions.

As mentioned earlier, owing to the heterogeneous nature of the functionally graded material, no exact solutions exist for the effective moduli and thermal expansion coefficient of a FGM coating even if the inclusion phase, be it metal or ceramic, can be taken as equal-sized spherical particles. Of course, the real microstructure of a FGM coating can be very complicated and all that we can have is a good approximate solution. In the following

sections, the effective thermomechanical properties of the coating given by the micromechanics solutions (9)–(12) will be used with the hope that they are accurate enough for practical purposes.

## 3. CRACKING UNDER MECHANICAL LOAD

Analyzed in this section is multiple cracking of the coating/substrate system as illustrated in Fig. 1 owing to a remotely applied uniform strain $\varepsilon_0$ in the $y$-direction. For simplicity, the parallel cracks are taken to be mode $I$, plane strain, equally spaced with spacing $2L$, and have the same length. For a uncracked coating/substrate system subjected to $\varepsilon_0$, the stress $\sigma_y$ in the coating is given by

$$\sigma_y(x) = \frac{\varepsilon_0 E(x)}{1-\nu^2(x)} \tag{13a}$$

and that in the substrate is uniform

$$\sigma_y = \frac{\varepsilon_0 E_m}{1-\nu_m^2}. \tag{13b}$$

The average stress $\sigma$ corresponding to the applied strain $\varepsilon_0$ is obtained readily as

$$\sigma = \frac{\varepsilon_0}{h+H}\left[\frac{HE_m}{1-\nu_m^2} + \int_0^h \frac{E(x)}{1-\nu^2(x)}\,dx\right], \tag{14}$$

where $H$ is the thickness of the substrate. In terms of this average stress $\sigma$, the energy release rate $\mathcal{G}$ for the multiple cracks can be normalized to give

$$\frac{\mathcal{G}\bar{E}_m}{\sigma^2 h} = \psi\left(\frac{a}{h}, \frac{L}{h}, f, n\right), \tag{15}$$

where $\psi$ is a non-dimensional function, $\bar{E}_m = E_m/(1-\nu_m^2)$ is the plane strain Young's modulus and the dependence of $\psi$ on $E_c/E_m$, $\nu_c$ and $\nu_m$ are left implicit.

Finite element calculations are carried out using the commercial code ABAQUS to obtain the energy release rate $\mathcal{G}$ for multiple cracks. Both the coating and the substrate are taken to be linear elastic; the metal substrate is assumed to be homogeneous, isotropic, with elastic moduli $E_m$, $\nu_m$ and thermal expansion coefficient $\alpha_m$. For all the calculations performed, the elastic moduli are taken to be $E_c/E_m = 3.0$, $\nu_m = 1/3$, $\nu_c = 0.2$, and the thermal expansion coefficient is assumed to be $\alpha_m = 1.3 \times 10^{-5}/^\circ\mathrm{C}$ for metal and $\alpha_c = 0.8 \times 10^{-5}/^\circ\mathrm{C}$ for ceramic. The thickness of the substrate $H$ is taken to be $300h$ where $h$ is the coating thickness. The FGM coating is divided into 100 layers, each layer is homogenous, isotropic with elastic moduli $E(x_i)$, $\nu(x_i)$ and thermal expansion coefficient $\alpha(x_i)$ where $x_i$ is the position of the middle plane of the layer measured from the coating surface. For example, $x_i$ for the tenth layer is $0.095h$. Clearly, in this finite element model the gradation is not continuous, nor is it in the real material. The model mimics the microstructure of a fine multilayered FGM coating, or an inclusion/matrix type FGM coating with gradation $g(x)$.

The coating/substrate system depicted in Fig. 1 is subjected to a remotely applied uniform strain $\varepsilon_0$ in the $y$-direction. Owing to translational symmetry of the parallel cracks,

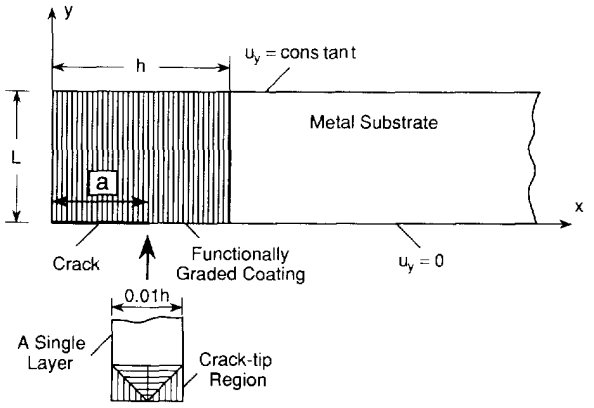


Fig. 6. The unit cell used in the finite element calculations for multiple cracking in the FGM coating. The coating is divided into 100 layers and the energy release rate $\mathcal{G}$ is calculated with the crack tip located in the middle of a layer.

only a unit cell with width $L$ shown in Fig. 6 needs to be considered in the finite element calculation. Specifically, the crack lies on $y = 0$, $0 \leqslant x \leqslant a$. For $a \leqslant x \leqslant h+H$, the displacement in the $y$-direction $u_y = 0$. The unit cell is constrained in such a way that the edge $y = L$ has a uniform displacement in the $y$-direction $u_y = \varepsilon_0 L$, where $\varepsilon_0$ is the applied strain. The energy release rate $\mathcal{G}$ is calculated with the crack tip located in the middle of a layer, as depicted in Fig. 6. Complications due to the singular behavior at the interfaces of two adjacent layers can thus be avoided.

Plotted in Fig. 7 is the normalized energy release rates $\mathcal{G}$ as a function of the crack length $a/h$ for multiple cracks with spacing $L/h = 10$. Results for cracks in a homogeneous metal ($f = 1.0$), a ceramic coating/metal substrate system ($f = 0.0$), and a FGM coating on a metal substrate with $f = 0.5$, $n = 1$ are shown for comparison. It is seen that when $a/h < 0.3$, the normalized energy release rate $\mathcal{G}\bar{E}_m/\sigma^2 h$ with the FGM coating is essentially the same as that with a ceramic coating. However, when $a/h > 0.4$, a significant reduction in $\mathcal{G}$ can be realized by using a FGM coating instead of a pure ceramic coating. The benefit of using FGM coatings is thus clearly demonstrated.

To uncover the influence of coating gradation on the crack driving force, systematic predictions are made for the energy release rates $\mathcal{G}$ corresponding to different coating gradation $g(x)$. Plotted in Fig. 8a are $\mathcal{G}\bar{E}_m/\sigma^2 h$ versus $x/h$ curves for $f = 0.5$, $L/h = 2$ for $n = 1, 2, 3, 4$ and 5. It is worth noticing that although there is a clear dependence of $\mathcal{G}$ on the value of $n$, the effect of $n$ (and therefore the coating gradation), is quite small. Note

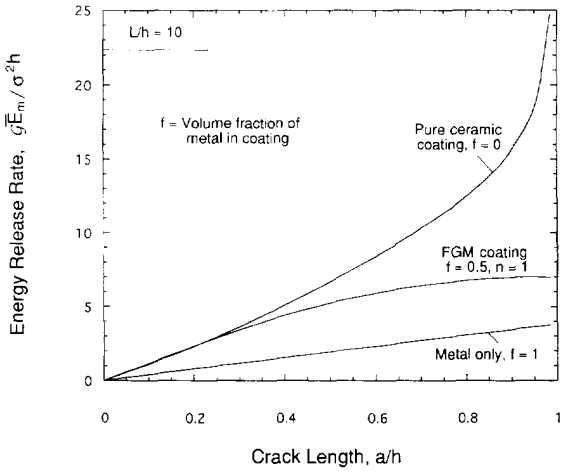


Fig. 7. Comparison of the normalized energy release rates $\mathcal{G}$ as a function of the crack length $a/h$ for multiple cracks in a homogeneous metal ($f = 1.0$), a ceramic-coating/metal-substrate system ($f = 0.0$), and a FGM coating on a metal substrate with $f = 0.5$, $n = 1$. The crack spacing is $L/h = 10$.

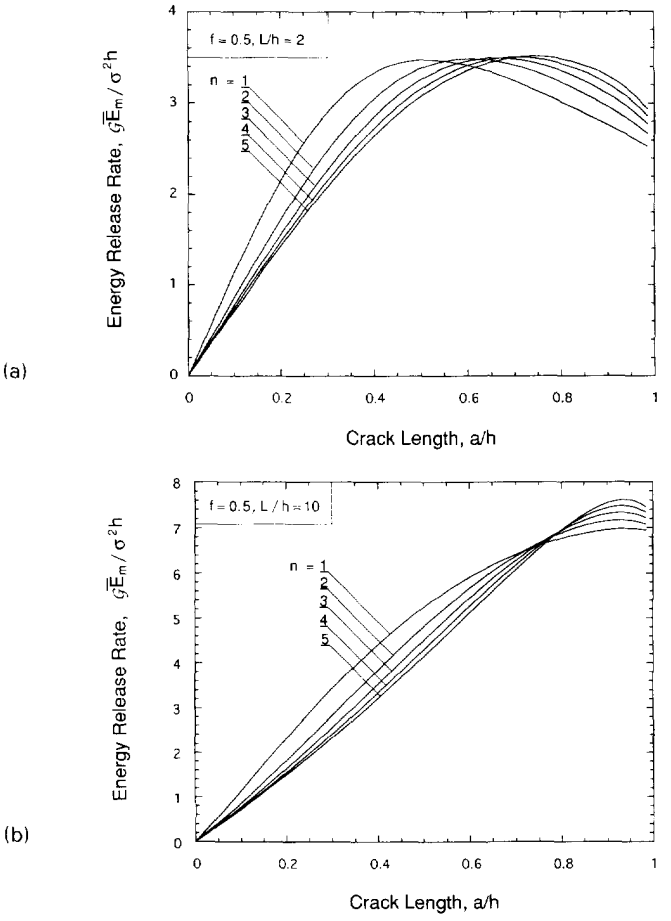


Fig. 8. The influence of coating gradation on the crack driving force $\mathcal{G}$. The normalized energy release rate $\mathcal{G}\bar{E}_m/\sigma^2 h$ is plotted against the crack length $a/h$ for FGM coatings with $f = 0.5$, $n = 1$, 2, 3, 4 and 5 with (a) crack spacing $L/h = 2$ and (b) crack spacing $L/h = 10$.

that $L/h = 2$ implies a large number of cracks in the coating, since the coating thickness $h$ is usually very small. When the crack spacing $L$ becomes larger, the effect of coating gradation is even smaller, as can be seen from Fig. 8b in which curves of $\mathcal{G}\bar{E}_m/\sigma^2 h$ versus $x/h$ for $f = 0.5$, $L/h = 10$, $n = 1$, 2, 3, 4, 5 are displayed. These results have important implications on the design of FGM coatings. Clearly, for a coating with a fixed metal volume fraction (say $f = 0.5$) subjected to mechanical loading, the energy release rate $\mathcal{G}$ is not very sensitive to the exact gradation of the FGM coating. Therefore, the requirement for the control of coating gradation in the processing can be less severe. In addition, an optimal design of the microstructure of a FGM coating can be conducted by mainly considering the thermomechanical properties, including thermal residual stresses and cracking under thermal loads.

To further quantify the fracture behavior of the FGM coating/metal substrate system, systematic finite element calculations are carried out for the energy release rate $\mathcal{G}$ corresponding to different crack spacings. The numerical results are summarized in Fig. 9a in which $\mathcal{G}\bar{E}_m/\sigma^2 h$ is plotted as a function of the crack length $a/h$ for $f = 0.5$, $n = 1$ for $L/h = 1$, 2, 5, 10, 20 and 50. For a FGM coating with $f = 0.5$ but with other values of $n (n \leqslant 5)$, the dependence of crack driving force $\mathcal{G}$ on crack spacing $L/h$ is expected to be similar to that shown in Fig. 9a. When crack density $h/L$ is small (or crack spacing $L/h$ is large), $\mathcal{G}$ increases monotonicly with crack length $a$. Thus, if the toughness of the coating $\Gamma$ is a constant (i.e. independent of the crack length $a$), the applied strain to cause crack growth always decreases as the crack length increases. However, when crack density $h/L$ is large, e.g. $h/L = 0.5$ ($L/h = 2$), there is a peak on the $\mathcal{G}\bar{E}_m/\sigma^2 h$ versus $a/h$ curve indicating that the cracks may arrest at a certain crack length. To further uncover the trends, the normalized energy release

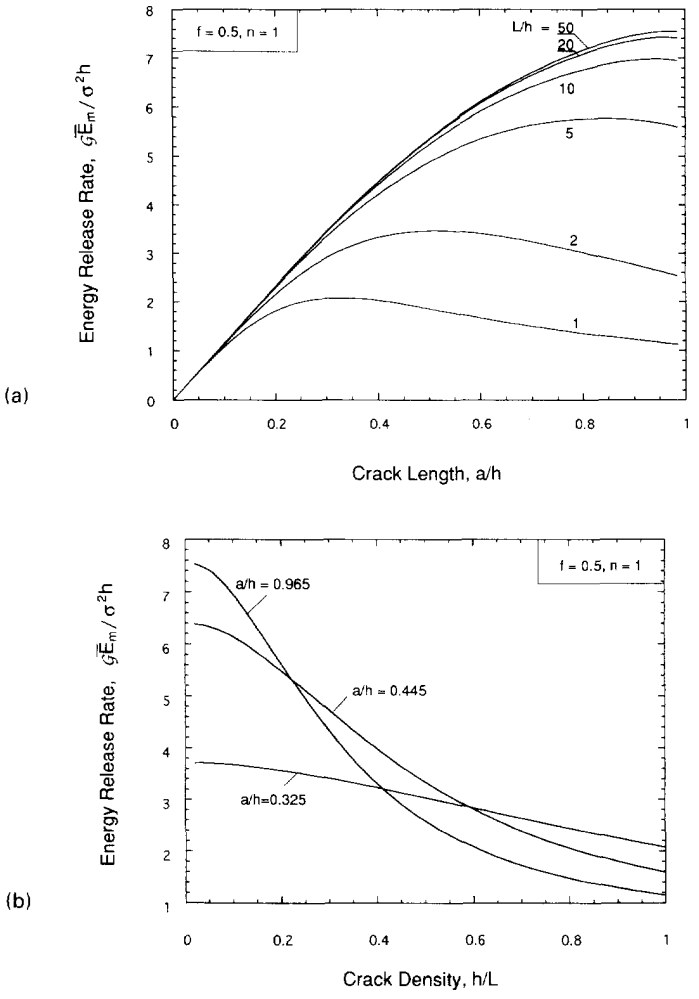


Fig. 9. The dependence of fracture driving force $\mathcal{G}$ on crack spacing. (a) The normalized energy release rate $\mathcal{G}\bar{E}_m/\sigma^2 h$ as a function of the crack length $a/h$ for cracks with spacing $L/h = 1, 2, 5, 10, 20$ and 50; (b) $\mathcal{G}\bar{E}_m/\sigma^2 h$ as a function of crack density $h/L$ for crack lengths $a/h = 0.325, 0.445, 0.965$.

rates $\mathcal{G}\bar{E}_m/\sigma^2 h$ are plotted in Fig. 9b as a function of the crack density $h/L$ for $a/h = 0.325$, 0.445, 0.965. It is seen that for short cracks (say, $a/h \leqslant 0.325$), a slight increase in applied strain will cause a large increase in crack density, since the $\mathcal{G}\bar{E}_m/\sigma^2 h$ versus $h/L$ curve is rather flat.

In some practical applications, it may be desirable to have 100% ceramic at the surface of a FGM coating. To provide guidance for the design of such coatings, calculations are carried out using the coating gradation $g(x) = (x/h)^n$ with $n = 0.5$, 1 and 2, as shown in Fig. 3b. Displayed in Fig. 10a and b are the corresponding effective Young's modulus $E(x)$ and Poission's ratio $\nu(x)$ obtained using micromechanics solutions (9)–(11). The dependence of the effective moduli $E$ and $\nu$ on the position $x$ in the FGM coating is again inherently similar to that of the local metal volume fraction $g(x)$.

Show in Fig. 11a are the normalized energy release rate $\mathcal{G}\bar{E}_m/\sigma^2 h$ as a function of crack length $a/h$ for $L/h = 2$ for $n = 0.5$, 1 and 2. Similar results are shown in Fig. 11b for cracks with spacing $L/h = 10$. The crack driving force $\mathcal{G}$ is higher when the metal volume fraction $f$ is lower, as might be expected. For multiple cracks with a relatively large spacing, say $L/h = 10$, $\mathcal{G}$ is monotonicly increasing with crack length until the crack tip is close to the coating/substrate interface. However, when crack spacing $L$ is small, say $L/h = 2$, $\mathcal{G}$ reaches its peak value at $a/h \approx 0.5$ indicating that crack arrest may occur at $a/h = 0.5$. This unique feature of functionally graded coatings is certainly beneficial in enhancing the performance of the coating/substrate system.

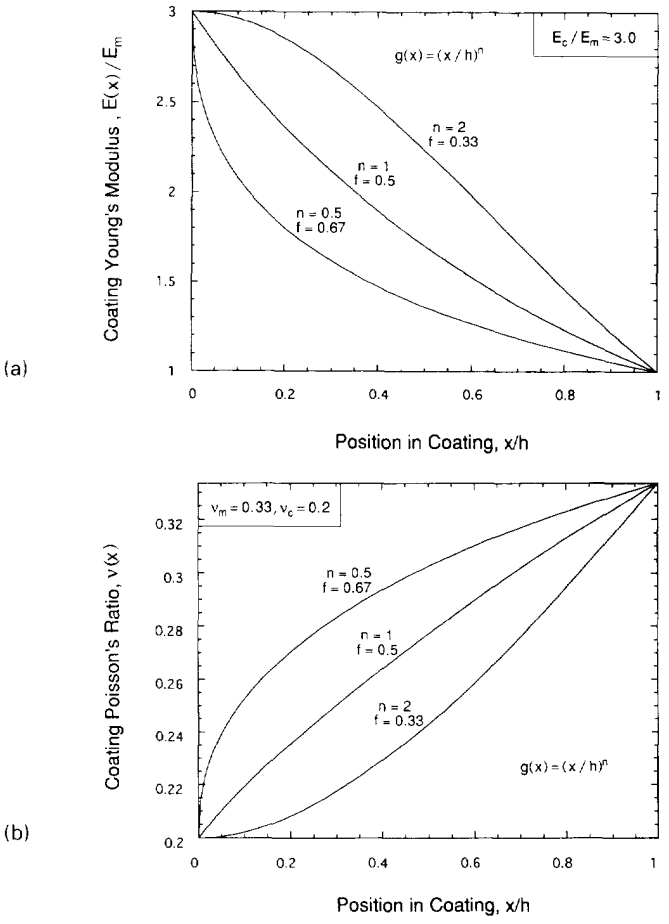


Fig. 10. Dependence of the effective elastic moduli and thermal expansion coefficient of the coating on the pure power-law coating gradation $g(x)$ given in eqn (4b). (a) Young's modulus $E(x)/E_m$ and (b) Poission's ratio $v(x)$.

## 4. CRACKING UNDER THERMAL LOAD

For a thin ceramic coating on a thick metal substrate under plane strain conditions, the residual stress $\sigma_T$ in the coating owing to thermal expansion mismatch is given by

$$\sigma_T = (\alpha_m - \alpha_c)(T - T_0)E_c/(1 - \nu_c^2), \tag{16a}$$

where $T$ is the current temperature and $T_0$ the stress-free temperature (i.e. the processing temperature). Since the thermal expansion coefficient for the ceramic $\alpha_c$ is usually lower than that for the metal, $\alpha_m$, $\sigma_T$ is compressive when $T < T_0$. For a thin functionally graded ceramic/metal coating on a thick metal substrate, the residual stress in the coating is given by

$$\sigma_T(x) = \frac{[\alpha_m - \alpha(x)](T - T_0)E(x)}{1 - \nu^2(x)}, \tag{16b}$$

where $\alpha(x)$, $E(x)$ and $\nu(x)$ are the effective properties of the FGM coating. Clearly, $\sigma_T(x)$ decreases with $x$ for coating gradations defined in (1); $\sigma_T(x) = 0$ at the interface. This implies that under the same applied tensile load, the FGM coating may be more prone to cracking at temperatures $T < T_0$ compared with a pure ceramic coating. On the other hand, when $T > T_0$, the tensile thermal stresses in a FGM coating are lower than that in a pure ceramic coating, so is the fracture driving force.

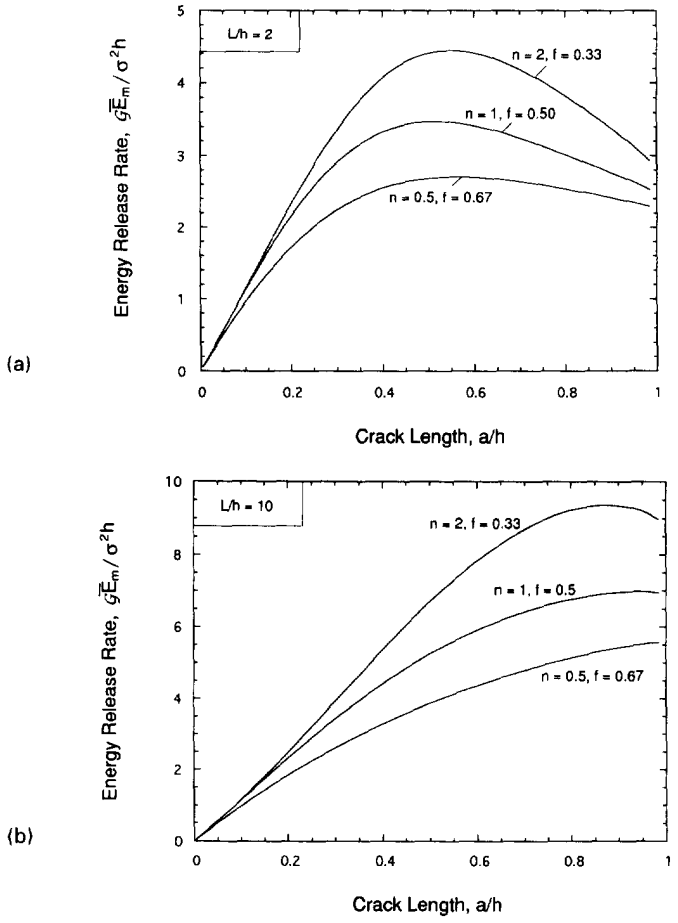


Fig. 11. The influence of coating gradation on the crack driving force $\mathcal{G}$. The normalized energy release rate $\mathcal{G}\bar{E}_m/\sigma^2 h$ is plotted against the crack length $a/h$ for FGM coatings with gradation $g(x) = (x/h)^n$, $n = 0.5$, 1 and 2. (a) Crack spacing $L/h = 2$; (b) crack spacing $L/h = 10$.

To quantify the fracture behavior of a FGM coating/metal substrate system under thermal load, finite element calculations are carried out based on the assumption that the coating gradation $g(x)$ obeys eqn (1), and that the elastic moduli and thermal expansion coefficient of the coating can be approximated by equations (9)–(12). It is assumed that the coating/substrate system has a constant temperature $T > T_0$ but is subjected to no mechanical load. The thermal expansion coefficient for the metal phase is taken to be $\alpha_m = 1.3 \times 10^{-5}/^\circ\text{C}$, and that for the ceramic phase is $\alpha_c = 0.8 \times 10^{-5}/^\circ\text{C}$. The actuarial temperature change $\Delta T = T - T_0$ used in the calculation is immaterial since the thermal stress $\sigma_T$ is proportional to $\Delta T$. The energy release rate $\mathcal{G}$ of multiple cracks in the coating is calculated using ABAQUS based on the configuration depicted in Fig. 6, and is normalized to give

$$\frac{\mathcal{G}\bar{E}_m}{\sigma_T^2 h} = \phi\left(\frac{a}{h}, \frac{L}{h}, f, n\right), \tag{17}$$

where $\phi$ is a nondimensional function, $\sigma_T$ is the thermal stress given in eqn (16a) and the dependence of $\phi$ on $E_c/E_m$, $\nu_c$ and $\nu_m$ are left implicit.

Displayed in Fig. 12 is the normalized energy release rate $\mathcal{G}\bar{E}_m/\sigma_T^2 h$ as a function of the crack length $a/h$ for a FGM coating with $f = 0.5$, $n = 1$ under thermal load. The corresponding result for a pure ceramic coating is also shown for comparison. It is seen that for $a/h < 0.15$, the difference is negligible. However, for crack lengths $a > 0.15h$, the reduction in $\mathcal{G}$ owing to the functional gradation of the coating can be very significant. For example, at $a/h = 0.5$, the value of $\mathcal{G}$ for the ceramic coating is about a factor of two higher

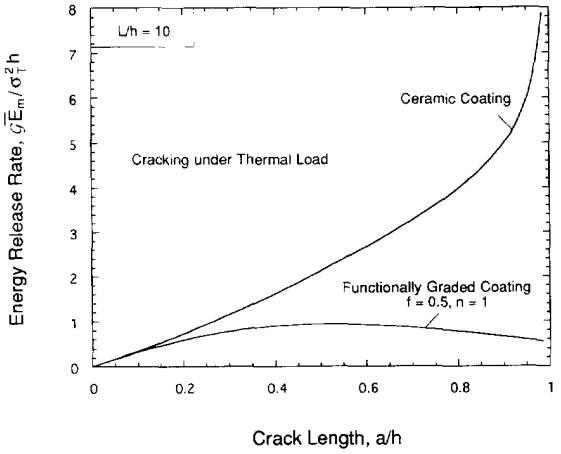


Fig. 12. Comparison of the thermal-load induced energy release rate $\mathcal{G}\bar{E}_m/\sigma_T^2 h$ as a function of the crack length $a/h$ for multiple cracks in a pure ceramic coating and in a FGM coating with $f = 0.5$, $n = 1$.

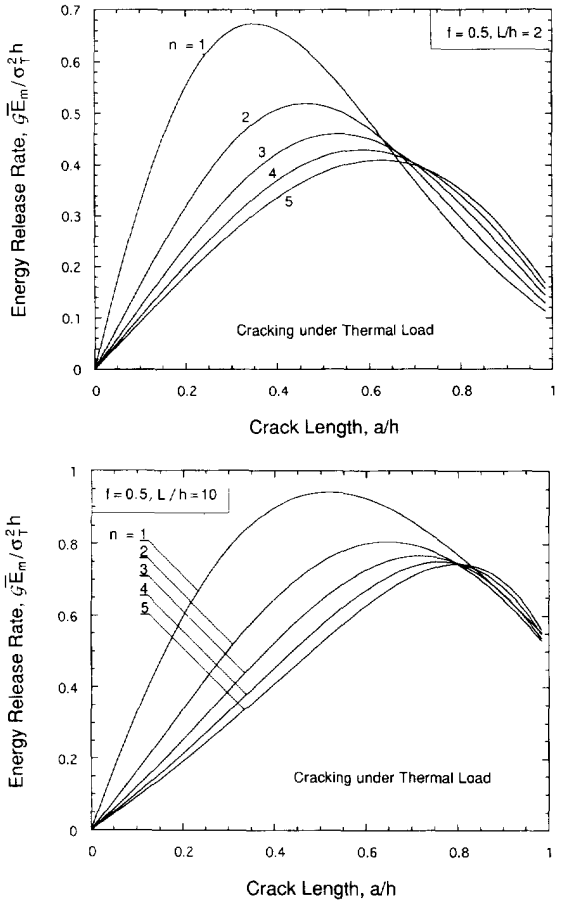


Fig. 13. The effect of coating gradation on the crack driving force $\mathcal{G}$ induced by thermal load. The normalized energy release rate $\mathcal{G}\bar{E}_m/\sigma_T^2 h$ is plotted against the crack length $a/h$ for FGM coatings with $f = 0.5$, $n = 1, 2, 3, 4$ and 5 with (a) crack spacing $L/h = 2$ and (b) crack spacing $L/h = 10$.

than that for the FGM coating. Obviously, when $T > T_0$, using a FGM coating is quite effective in reducing fracture damage in the coating under thermal load.

To uncover the effect of coating gradation on the fracture behavior, calculations are carried out for coatings with $f = 0.5$, $n = 1$, 2, 3, 4 and 5 where $n$ is the exponent of the power-law type coating gradation defined in eqn (1). Shown in Fig. 13a are curves of

$\mathcal{G}\bar{E}_m/\sigma_T^2 h$ versus $a/h$ for cracks with spacing $L/h = 2$. Unlike the fracture behavior under applied mechanical load, the dependence of $\mathcal{G}$ on coating gradation is seen to be quite strong. In addition, a peak appears on each curve; its value and the corresponding crack length depend on the value of $n$. Consequently, crack arrest may occur under a constant temperature field even if the toughness of the FGM coating does not increase with crack length. When $a/h < 0.6$, the linear gradation ($n = 1$) gives rise to relatively high values of $\mathcal{G}$, while the nonlinear gradations ($n \geqslant 2$) result in somewhat lower values of $\mathcal{G}$. For crack lengths $a < 0.6h$, the higher the value of $n$, the lower the crack driving force $\mathcal{G}$. For $a/h > 0.7$, the opposite trend is true, but the difference in $\mathcal{G}$ is rather small. Similar trends are true for cracks with spacing $L/h = 10$, as can be seen from Fig. 13b, but the crack length beyond which the influence of coating gradation is small becomes $a/h = 0.8$.

To further quantify the crack driving force for multiple cracking in the FGM coating owing to thermal load, calculations are carried out for the FGM coating with $f = 0.5$, $n = 1$ having cracks with spacing $L/h = 1, 2, 5, 10, 20$ and 50. The numerical results for $\mathcal{G}$ are displayed in Fig. 14. For each crack spacing considered, initially the value of $\mathcal{G}$ increases with crack length. It then reaches a maximum value and decreases with crack length. The crack length at which $\mathcal{G}$ has its peak value increases with the crack spacing $L/h$ which indicates that under thermal load, as crack density becomes large, the parallel cracks tend to arrest at a relatively small crack length.

## 5. CRACKING UNDER MECHANICAL AND THERMAL LOADS

Now consider cracking of the FGM coating under a combination of thermal load $\sigma_T$ and mechanical load $\sigma > 0$. Depending on the current temperature $T$ as compared with the stress-free temperature $T_0$, $\sigma_T$ can be positive ($T > T_0$) or negative ($T < T_0$). Since the coating/substrate system under study is taken to be linear, the total stress intensity factor $K$ at the crack tip can be given by

$$K = K_\sigma + K_T, \tag{18}$$

where $K_\sigma$ is the stress intensity factor owing to applied mechanical load and $K_T$ is that owing to the thermal load. From fracture mechanics analysis

$$K(a) = \sqrt{\mathcal{G}(a)\bar{E}(a)}, \tag{19}$$

where $\mathcal{G}$ is the total energy release rate and $\bar{E} = E/(1-\nu^2)$ is the plane strain Young's modulus for the FGM coating evaluated at $x = a$. Consequently, for multiple cracks in the FGM coating/metal substrate system shown in Fig. 1, $K_\sigma$ can be given in a non-dimensional form

$$\frac{K_\sigma}{\sigma\sqrt{h}} = \sqrt{\frac{\mathcal{G}\bar{E}_m}{\sigma^2 h}\frac{\bar{E}(a)}{\bar{E}_m}}, \tag{20}$$

where the normalized energy release rate $\mathcal{G}\bar{E}_m/\sigma^2 h = \psi(a/h, L/h, f, n)$ is displayed numerically in Figs 8, 9 and 11. Similarly, the stress intensity factor $K_I$ can be given by

$$\frac{K_T}{\sigma_T\sqrt{h}} = \sqrt{\frac{\mathcal{G}\bar{E}_m}{\sigma_T^2 h}\frac{\bar{E}(a)}{\bar{E}_m}}, \tag{21}$$

where $\mathcal{G}\bar{E}_m/\sigma_T^2 h = \phi(a/h, L/h, f, n)$ is presented numerically in Figs 13 and 14. Note that if $\alpha_m > \alpha_c$ and $T < T_0$, $\sigma_T$ as defined in eqn (17) is negative, so is $K_T$.

The total stress intensity factor $K$ has the form

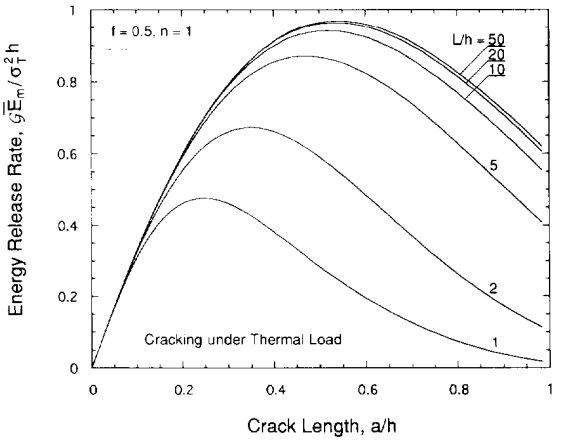


Fig. 14. The dependence of fracture driving force $\mathcal{G}$ on crack spacing. The normalized energy release rate $\mathcal{G}\bar{E}_m/\sigma_T^2 h$ owing to thermal load is plotted as a function of the crack length $a/h$ for cracks with spacing $L/h = 1, 2, 5, 10, 20$ and 50.

$$\frac{K}{\sigma\sqrt{h}} = \left[\sqrt{\psi} + \frac{\sigma_T}{\sigma}\sqrt{\phi}\right]\sqrt{\frac{\bar{E}(a)}{\bar{E}_m}}. \tag{22}$$

Note again that when $\alpha_m > \alpha_c$ and $T < T_0$, $\sigma_T/\sigma < 0$. Thus, for certain values of $\sigma_T/\sigma$, the total stress intensity factor $K$ can become negative which implies that crack growth in the FGM coating is prohibited. To illustrate, in Fig. 15a, The normalized total stress intensity factor $K/\sigma\sqrt{h}$ is plotted against the crack length $a/h$ for a coating with gradation $f = 0.5$, $n = 1$ and with crack spacing $L/h = 2$. The load ratio $\sigma_T/\sigma$ is taken to be $-4$, $-3$, $-2$, $-1$, 0, 1 and 2. It is seen that for $\sigma_T/\sigma = -4$, the total stress intensity factor $K$ is negative for almost all values of crack length $a$. This implies that the coating can sustain certain applied strain without cracking. As an example, consider a FGM coating with $\alpha_m = 1.3 \times 10^{-5}/°C$, $\alpha_c = 0.8 \times 10^{-5}/$ C, $T - T_0 = -800$ C, $E_c = 250$ GPa, $\nu_c = 0.2$. We thus have from eqn (17) $\sigma_T = -1.04$ GPa, and no parallel cracks with spacing $L/h = 2$ can grow in such a coating under applied strain that gives rise to $\sigma = 250$ MPa. The crack length below which $K$ is negative decreases with increasing $\sigma_T/\sigma$, as might be expected. Roughly speaking, for $\sigma_T/\sigma > -2$, $K$ is always positive for the present case. It is also clear that for $T > T_0$, i.e. $\sigma_T/\sigma > 0$, the stress intensity factor can be significantly higher than that without thermal load. Similar features are true for cracks with spacing $L/h = 10$, as can be seen from Fig. 15b.

To further demonstrate the fracture behavior of a FGM coating as compared with that of a pure ceramic coating, in Fig. 16, the total stress intensity factor $K$ is plotted as a function of crack length $a$ for cracks in a FGM coating with $f = 0.5$, $n = 1$ and in a pure ceramic coating. The crack spacing is taken to be $L/h = 10$. With a given applied strain (therefore a fixed $\sigma$), if the temperature is low such that $\sigma_T/\sigma = -3$, the cracks will not grow in the pure ceramic coating but may grow in the FGM coating if the crack length is large. However, if the temperature is high such that $\sigma_T/\sigma \geqslant -1$, the stress intensity factor $K$ for cracks in the pure ceramic coating can be much larger than that corresponding to the FGM coating. It is again clear that the use of FGM coating can be very advantageous.

## 6. CONCLUDING REMARKS

Functionally graded coatings are potentially very attractive to a number of applications including as thermal barrier coatings and wear resistant coatings. Compared with pure ceramic coatings, FGM coatings can have high hardness and oxidation resistance at the surface, but with much lower thermal residual stresses. The material gradation in such coatings provides a new dimension in optimizing the coating performance.

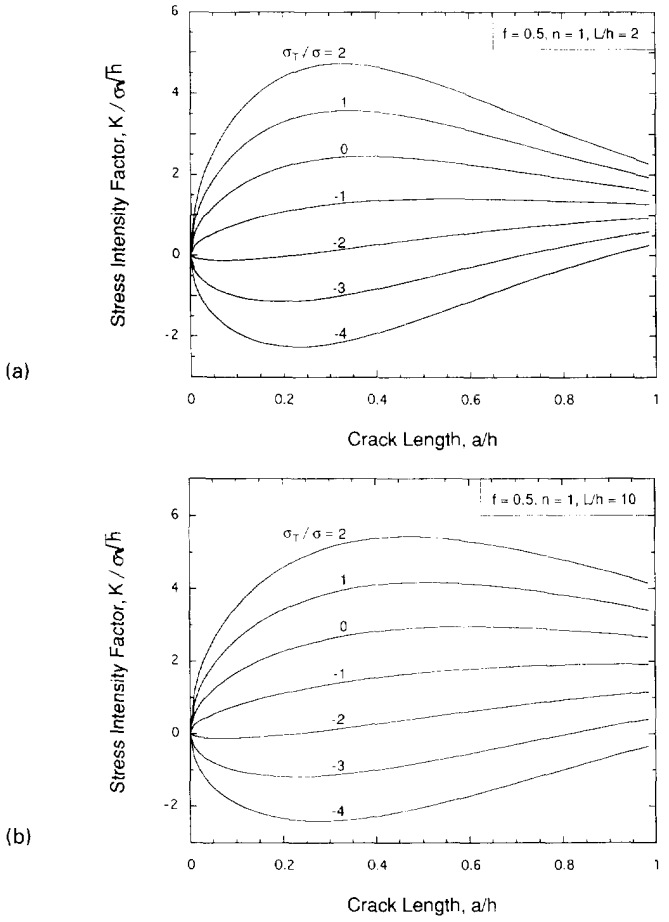


Fig. 15. The fracture driving force due to combined thermal and mechanical loads with $\sigma_T/\sigma = -4$, $-3$, $-2$, $-1$, 0, 1 and 2. The normalized total stress intensity factor $K/\sigma\sqrt{h}$ is plotted as a function of the crack length $a/h$ for coatings with gradation $f = 0.5$, $n = 1$ and with (a) crack spacing $L/h = 2$, (b) crack spacing $L/h = 10$.

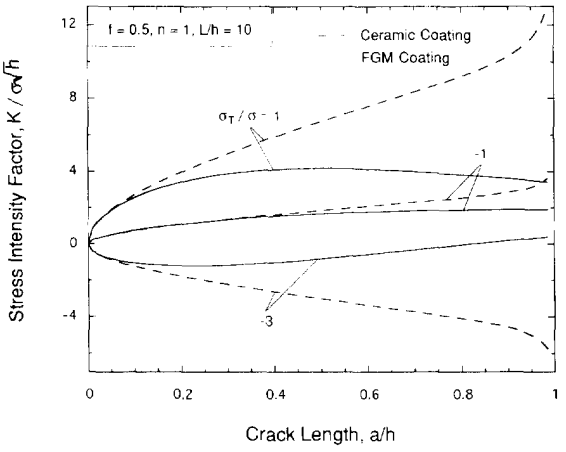


Fig. 16. Comparison of the fracture behavior of a FGM coating and a pure ceramic coating under combined thermal and mechanical loads with $\sigma_T/\sigma = -3$, $-1$, and 1. The normalized total stress intensity factor $K/\sigma\sqrt{h}$ is plotted as a function of the crack length $a/h$ for coatings with gradation $f = 0.5$, $n = 1$.

Owing to the material gradation, the FGM coating is inherently heterogeneous, and the microstructure–performance relationship is very complex. More material parameters come into play, but few models are available to guide the gradation design. In order to

realize the potential of FMG coatings, recently a number of researchers, especially Erdogan and his coworkers, have been carrying out mechanics analyses of the fracture behavior of the coating and the coating/substrate interface. The present work focuses on the dependence of fracture driving force on the coating gradation, aiming to gain a better understanding of the microstructure–performance relation of the FGM coatings. The coating gradation is characterized by the local volume fraction of metal $g(x)$ which has a power-law type dependence on position $x$. Systematic finite element calculations are made for the energy release rate of multiple cracks in the coating as determined by the coating gradation, crack length, and the crack density; both mechanical and thermal loads are considered. It is found that compared with the pure ceramic coating, gradation of the coating can significantly reduce the crack driving force. It is also found that under mechanical loading the effect of different gradations on the crack driving force is relatively small. However, under thermal loading the influence of coating gradation can be significant.

The results obtained in this work have important implications to the design of FGM coatings. First, for a FGM coating with equal volume fractions of metal and ceramic (i.e. $f = 0.5$) under mechanical loading, the requirement for the control of coating gradation in the processing can be less severe, since the energy release rate $\mathcal{G}$ is not sensitive to the exact gradation. Thus, an optimal design of the microstructure of a FGM coating can be conducted by mainly considering the thermomechanical properties, including thermal residual stresses and cracking under thermal loads. Second, for a FGM coating with $f = 0.5$ subjected to a temperature field $T > T_0$, the linear gradation gives rise to the highest fracture driving force $\mathcal{G}$, especially when the crack length is small. This implies that ceramic content in the coating should be rather uniform near the coating surface, and decrease rapidly near the coating/substrate interface.

The toughness of a FGM coating is most likely to increase with crack length owing to plastic deformation of the metal phase in the coating and various crack bridging mechanisms (Bao and Hui, 1990; Bao and Suo, 1992; Bao and Zok, 1993). Nonlinear fracture mechanics analysis is therefore needed to predict the $R$-curve behavior of the FGM coating. It is possible to make a complete assessment of the coating gradation/performance relationship only when the $R$-curve behavior of the coating is obtained.

*Acknowledgment* This work was supported in part by NSF through a Research Initiation Award MSS 9210250 to GB.

## REFERENCES

Aboudi, J., Arnold, S. M. and Pindera, M. J. (1994). Response of functionally graded composites to thermal gradients. *Compos. Engng* **4**, 1–18.

Bao, G. and Hui, C. Y. (1990). Effects of interface debonding on the toughness of ductile-particle reinforced ceramics. *Int. J. Solids Structures* **26**, 631–642.

Bao, G. and Suo, G. (1992). Remarks on crack bridging concepts. *Appl. Mech. Rev.* **45**, 355–366.

Bao, G. and Zok, F. (1993). On the strength of ductile particle reinforced brittle matrix composites. *Acta Metall. Mater.* **41**, 3515–3524.

Christensen, R. M. (1991). *Mechanics of Composite Materials*. Krieger, Malabar, FL.

Christensen, R. M. and Lo, K. H. (1979). Solutions for effective shear properties in three phase sphere and cylinder models. *J. Mech. Phys. Solids* **27**, 315–330.

Delale, F. and Erdogan, F. (1983). The crack problem for a nonhomogeneous plane. *J. Appl. Mech.* **50**, 609–614.

Delale, F. and Erdogan, F. (1988). On the mechanical modeling of the interface region in bonded half-planes. *J. Appl. Mech.* **55**, 317–324.

Drake, J. T., Williamson and R. L., Rabin (1993). Finite element analysis of thermal residual stresses at graded ceramic–metal interfaces. Part II. Interface optimization for residual stress reduction. *J. Appl. Phys.* **74**, 1321–1326.

Dvorak, G. and Zuiker, J. (1994). The effective properties of functionally graded composites I. Extension of the Mori–Tanaka method to linearly varying fields. *Compos. Engng* **4**, 19–35.

Erdogan, F. (1985). The crack problem for bonded nonhomogeneous materials under antiplane shear loading. *J. Appl. Mech.* **52**, 823–828.

Erdogan, F. and Wu, B. H. (1993). Analysis of FGM specimens for fracture toughness testing. In *Ceramic Transactions, Functionally Gradient Materials* (Edited by J. B. Hole *et al.*), Vol. 34, pp. 39–46. American Ceramic Society, Westerville, Ohio.

Gecit, M. R. (1979). Fracture of a surface layer bonded to a half space. *Int. J. Engng Sci.* **17**, 287–295.

Giannakopoulos, A. E., Suresh, S., Finot, M. and Olsson, M. (1994). Elastoplastic analysis of thermal cycling: Layered materials with compositional gradients. *Acta Metall. Mater.* In press.

Hashin, Z. (1962). The elastic moduli of heterogeneous materials. *J. Appl. Mech.* **29**, 143–150.

Hu, M. S. and Evans, A. G. (1989). The cracking and decohesion of thin films on ductile substrate. *Acta Metall.* **37,** 917–925.

Hutchinson, J. W. and Suo, Z. (1992). Mixed mode cracking in layered materials. In *Advances in Applied Mechanics* (Edited by J. W. Hutchinson and T. Y. Wu), Vol. 29, pp. 63–191. Academic Press, New York.

Jin, Z.-H. and Noda, N. (1993a). An internal crack parallel to the boundary of a nonhomogeneous half plane under thermal loading. *Int. J. Engng Sci.* **31,** 793–806.

Jin, Z.-H. and Noda, N. (1993b). Minimization of thermal stress intensity factors for a crack in a metal-ceramics mixture. In *Ceramic Transactions, Functionally Gradient Materials* (Edited by J. B. Hole *et al.*), Vol. 34, pp. 47–54. American Ceramic Society, Westerville, Ohio.

Jin, Z.-H. and Noda, N. (1994a). Crack-tip singular fields in functionally gradient materials. *J. Appl. Mech.* **61,** 738–740.

Jin, Z.-H. and Noda, N. (1994b). Transient thermal stress intensity factors for a crack in a semi-infinite plate of a functionally gradient material. *Int. J. Solids Structures* **31,** 203–218.

Lannutti, J. J. (1994). Functionally graded materials: properties, potential and design guidelines. *Compos. Engng* **4,** 81–94.

Niino, M, Hirai, T. and Watanabe, R. (1987). The functionally gradient materials. *J. Jap. Soc. Compos. Mater.* **13,** 257.

Noda, N. and Jin, Z.-H. (1993). Thermal stress intensity factors for a crack in a strip of a functionally gradient material. *Int. J. Solids Structures* **30,** 1039–1056.

Takahashi, H. and Hashida, T. (1990). Development of an evaluation method of functionally gradient materials. *JSME Int. J.* **33,** 281–287.

Varna, J. and Berglund, L. A. (1994). Thermo-elastic properties of composite laminates with transverse cracks. *J. Compos. Tech. Rev.* **16,** 77–87.

Wang, A. S. D. (1984). Fracture mechanics of sublaminate cracks in composite materials. *J. Compos. Tech. Rev.* **6,** 45–62.

Wang, A. S. D., Chou, P. S. and Lei, S. C. (1984). A stochastic model for the growth of matrix cracks in composite laminates. *J. Compos. Mater.* **18,** 239–254.

Williamson, R. L., Rabin, B. H. and Drake, J. T. (1993). Finite element analysis of thermal residual stresses at graded ceramic–metal interfaces. Part I. Model description and geometrical effects. *J. Appl. Phys.* **74,** 1310–1320.